

Estimating Liquefaction-Induced Lateral Displacements Using the Standard Penetration Test or Cone Penetration Test

G. Zhang¹; P. K. Robertson, M.ASCE²; and R. W. I. Brachman³

Abstract: A semiempirical approach to estimate liquefaction-induced lateral displacements using standard penetration test (SPT) or cone penetration test (CPT) data is presented. The approach combines available SPT- and CPT-based methods to evaluate liquefaction potential with laboratory test results for clean sands to estimate the potential maximum cyclic shear strains for saturated sandy soils under seismic loading. A lateral displacement index is then introduced, which is obtained by integrating the maximum cyclic shear strains with depth. Empirical correlations from case history data are proposed between actual lateral displacement, the lateral displacement index, and geometric parameters characterizing ground geometry for gently sloping ground without a free face, level ground with a free face, and gently sloping ground with a free face. The proposed approach can be applied to obtain preliminary estimates of the magnitude of lateral displacements associated with a liquefaction-induced lateral spread.

DOI: 10.1061/(ASCE)1090-0241(2004)130:8(861)

CE Database subject headings: Liquefaction; Lateral displacement; Earthquakes; Sand; In situ tests.

Introduction

Earthquake shaking may trigger the liquefaction of a saturated sandy soil in the ground. During past major earthquakes, enormous damage to engineered structures and lifelines has been caused by liquefaction-induced ground failures (e.g., Hamada and O'Rourke 1992). Generally, liquefaction-induced ground failures include flow slides, lateral spreads, ground settlements, ground oscillation, and sand boils. Lateral spreads are the pervasive types of liquefaction-induced ground failures for gentle slopes or for nearly level (or gently inclined) ground with a free face (e.g., river banks, road cuts). This paper focuses on the estimation of lateral displacements associated with liquefaction-induced lateral spreads.

Several methods have been proposed to estimate liquefaction-induced lateral ground displacements including numerical models, laboratory tests, and field-test-based methods. Challenges associated with sampling loose sandy soils limit the applications of numerical and laboratory testing approaches in routine practice. Field-test-based methods are likely best suited to provide simple

direct methods to estimate liquefaction-induced ground deformations for low-to medium-risk projects and to provide preliminary estimates for high-risk projects.

Methods using standard penetration test (SPT) data are available for estimating lateral displacements in a liquefaction-induced lateral spread (Rauch and Martin 2000; Bardet et al. 2002; Youd et al. 2002). These methods are empirical and do not incorporate the extensive knowledge gained from laboratory studies of liquefaction. Further, even though the cone penetration test (CPT) has greater repeatability and reliability, and provides a continuous profile compared with other field tests, no CPT-based method to estimate liquefaction-induced lateral displacements is currently available.

The objective of this paper is to present an approach for estimating liquefaction-induced lateral displacements using SPT or CPT data. The approach combines available SPT- or CPT-based methods to estimate liquefaction potential with laboratory test results for clean sand to estimate the potential maximum cyclic shear strains for saturated sandy soils under seismic loading. Case history data are used to develop empirical correlations for lateral displacement for: (1) gently sloping ground without a free face, (2) level ground with a free face, and (3) gently sloping ground with a free face.

Mechanism of Liquefaction-Induced Lateral Spreads

One-*g* shake table tests (e.g., Sasaki et al. 1991; Yasuda et al. 1992) and centrifuge model tests (e.g., Abdoun 1997; Taboada-Urtzuastegui and Dobry 1998) have been conducted to investigate the mechanisms of liquefaction-induced ground lateral spreads. These tests generally support the hypothesis that lateral spreads result from distributed residual shear strains throughout the liquefied layers. The residual shear strains in liquefied layers are primarily a function of: (1) maximum cyclic shear strains γ_{\max} , and (2) biased in situ static shear stresses. In this paper, γ_{\max} refers to the maximum amplitude of cyclic shear strains that

¹Project Engineer, EBA Engineering Consultants Ltd., 14940-123 Ave., Edmonton AB, Canada T5V 1B4.

²Associate Vice President (Research/Industry) and Professor, Dept. of Geotechnical Engineering, Univ. of Alberta, Edmonton AB, Canada T6G 2G7.

³Assistant Professor, GeoEngineering Centre at Queen's-RMC, Queen's Univ., Kingston ON, Canada K7L 3N6 (corresponding author). E-mail: brachman@civil.queensu.ca

Note. Discussion open until January 1, 2005. Separate discussions must be submitted for individual papers. To extend the closing date by one month, a written request must be filed with the ASCE Managing Editor. The manuscript for this paper was submitted for review and possible publication on December 19, 2001; approved on December 21, 2003. This paper is part of the *Journal of Geotechnical and Geoenvironmental Engineering*, Vol. 130, No. 8, August 1, 2004. ©ASCE, ISSN 1090-0241/2004/8-861-871/\$18.00.

are induced during undrained cyclic loading for a saturated sandy soil without biased static shear stresses in the direction of cyclic loading. Biased in situ static shear stresses are mainly controlled by ground geometry at the site (e.g., ground slope, free face height, and the distance to a free face). The thickness of liquefied layers will also influence the magnitude of lateral displacements, with greater lateral displacements for thicker liquefied layers. Both γ_{\max} and the thickness of liquefied layers are affected by soil properties and earthquake characteristics.

Estimation of Maximum Shear Strains from Standard Penetration Test or Cone Penetration Test Data

Maximum Cyclic Shear Strains of Clean Sands from Laboratory Tests

Nagase and Ishihara (1988) conducted cyclic simple shear tests on saturated loose, medium-dense, and dense samples of clean Fuji River sand under loading conditions without biased static shear stresses. Based mainly on these laboratory tests, Ishihara and Yoshimine (1992) established the relationship between the γ_{\max} and the factor of safety (FS) against liquefaction for different relative densities (D_r) of clean sands. Modification of this relationship is required to account for dilative response of the soil that may restrict the development of shear strains. Evidence of soil dilative response at large shear strains has been observed in undrained cyclic laboratory tests, one- g shake table studies, centrifuge experiments, and in situ seismic responses (Elgamal et al. 1998). Seed (1979) postulated that only a limited amount of shear strain could be developed for sand at any given relative density, regardless of the number of stress cycles applied, and that further increases in strain could be difficult to achieve unless the full undrained resistance of the soil was exceeded. In this study, the relationship between γ_{\max} and FS developed by Ishihara and Yoshimine (1992) were modified by limiting the maximum shear strains as proposed by Seed (1979).

Factor of Safety and Relative Density from the Standard Penetration Test and Cone Penetration Test

Both the factor of safety against liquefaction and relative density (D_r) are needed to estimate γ_{\max} of a clean sand for a given earthquake. FS can be evaluated from liquefaction potential analysis using the SPT- or CPT-based methods summarized by Youd et al. (2001), hereafter referred to as the NCEER (National Center for Earthquake Engineering Research) SPT-based method or the NCEER CPT-based method.

Relative densities may be estimated from correlations with either SPT or CPT results. A modified version of Meyerhof's (1957) correlation was used to estimate relative densities of a clean sand from SPT blow counts

$$D_r = 16 \cdot \sqrt{(N_1)_{78}} = 14 \cdot \sqrt{(N_1)_{60}} \quad [(N_1)_{60} \leq 42] \quad (1)$$

where D_r = relative density of a clean sand as a percentage; $(N_1)_{60}$ = normalized SPT N value corrected for the rod energy ratio (60% reference energy), overburden effective stress (100 kPa reference effective stress), rod length, borehole diameter, and sampling method, as discussed in Youd et al. (2001); and $(N_1)_{78}$ is equal to $(N_1)_{60}/1.3$. Generally, the calculated relative density using Eq. (1) is reasonably consistent with those calculated using other available correlations (Seed 1979; Skempton 1986; Kul-

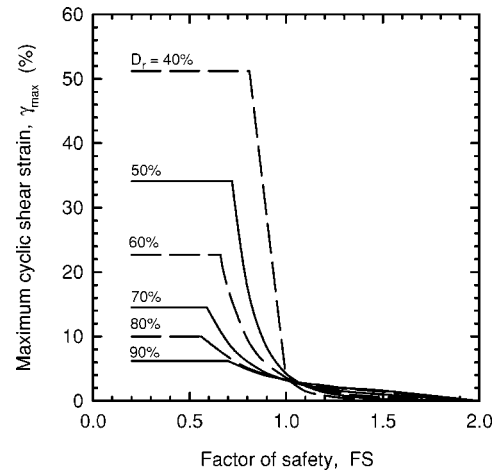


Fig. 1. Relationship between maximum cyclic shear strain and factor of safety for different relative densities D_r for clean sands [based on data from Ishihara and Yoshimine (1992) and Seed (1979)]

hawy and Mayne 1991) for a given SPT N value and is applicable for relatively young (<5,000 years) or normally consolidated sand.

The correlation between D_r and cone tip resistance (q_c) of Tatsuoka et al. (1990) was used

$$D_r = -85 + 76 \log(q_{c1N}) \quad (q_{c1N} \leq 200) \quad (2)$$

where q_{c1N} = normalized CPT tip resistance corrected for effective overburden stresses corresponding to 100 kPa (Robertson and Wride 1998). This correlation provides slightly smaller and more conservative estimates of relative density than the correlation by Jamiolkowski et al. (1985) when q_{c1N} is less than about 100.

Correction for Grain Characteristics

The relationship between γ_{\max} and FS proposed by Ishihara and Yoshimine (1992) was developed based on laboratory test results on clean sands. The equivalent clean sand normalized SPT N value, $(N_1)_{60cs}$, and the equivalent clean sand normalized CPT penetration resistance, $(q_{c1N})_{cs}$, is used to account for the effect of grain characteristics (or fines content) on SPT N values or CPT soundings in evaluating liquefaction potential of silty sands (Youd et al. 2001). In this work, $(N_1)_{60cs}$ or $(q_{c1N})_{cs}$, was also applied to quantify the effect of grain characteristics (or fines content) on SPT N values or CPT soundings in estimating γ_{\max} . The parameter, $(N_1)_{60cs}$ or $(q_{c1N})_{cs}$ for a silty sand, can then be treated as the SPT N value or CPT cone tip resistance for a clean sand and be used directly to estimate γ_{\max} . This assumes that the effect of grain characteristics or fines content on lateral spreading is similar to its effect on liquefaction triggering. This assumption will be discussed further later in this paper.

Fig. 1 shows the relationships used in this study between γ_{\max} and FS for different D_r . With either SPT or CPT data and the parameters for a given earthquake, $(N_1)_{60cs}$ or $(q_{c1N})_{cs}$ and FS for sandy soils can be estimated from the liquefaction potential analysis using the NCEER SPT- or CPT-based method. An estimate of γ_{\max} can then be obtained from Fig. 1 for every reading in the SPT or CPT results.

Lateral Displacement Index

Integrating the calculated γ_{\max} values with depth will produce a value that is defined as the lateral displacement index (LDI)

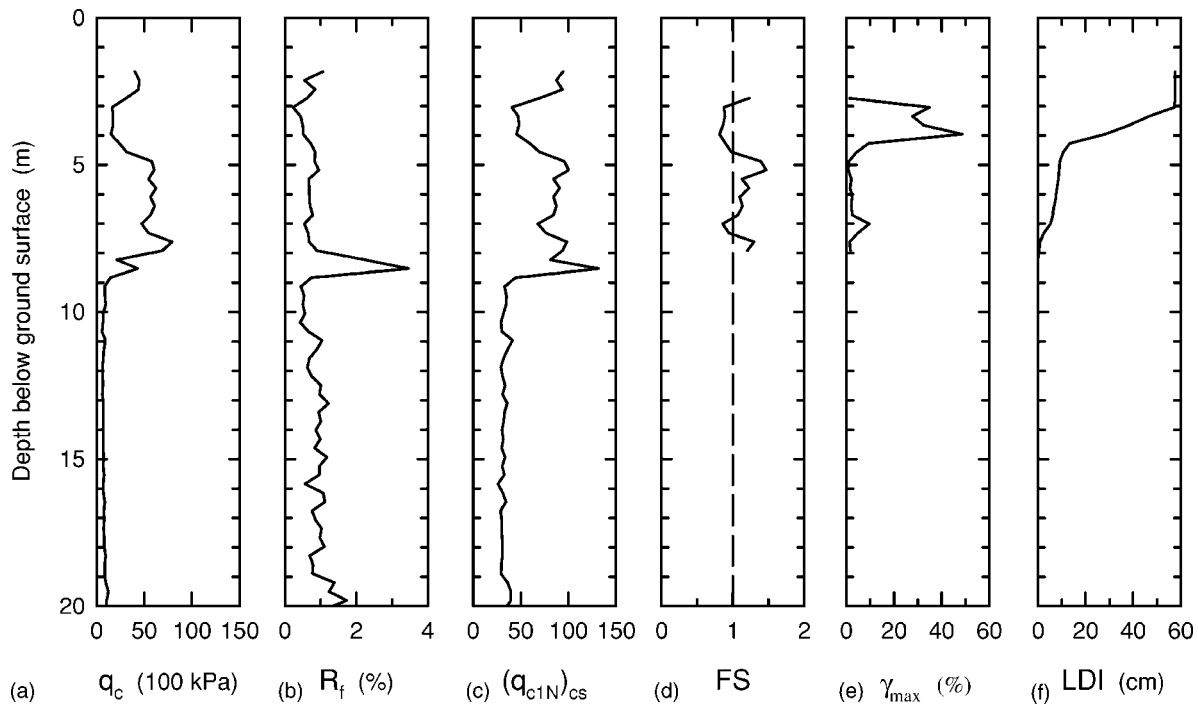


Fig. 2. Example plots illustrating the major steps for calculating the lateral displacement index (LDI) using the CPT-based approach

$$LDI = \int_0^{Z_{\max}} \gamma_{\max} dz \quad (3)$$

where Z_{\max} = maximum depth below all the potential liquefiable layers with a calculated $FS < 2.0$. However, evaluation of liquefaction at depths greater than 23 m is beyond the range where the NCEER CPT and SPT methods have been verified and where routine applications should be applied (Youd et al. 2001).

Figs. 2(a–f) illustrate the major steps to calculate LDI using CPT data. Figs. 2(a and b) show the CPT tip resistance (q_c) and sleeve friction ratio (R_f), which can be calculated directly from CPT soundings. Based mainly on q_c and R_f , the equivalent clean sand normalized tip resistance ($(q_{c1N})_{cs}$) can be calculated using the NCEER CPT-based method, Fig. 2(c). FS can be estimated using the NCEER CPT-based method with $(q_{c1N})_{cs}$ and the design earthquake parameters [Fig. 2(d)]. Note that in Fig. 2(d), a soil layer below 8 m is estimated to be a nonliquefiable clayey soil based on CPT data and is assigned a large value of FS (> 2.0). Fig. 2(e) shows γ_{\max} as estimated from the relationships in Fig. 1. Finally, the lateral displacement index (LDI) can be calculated by integrating the γ_{\max} with depth [Fig. 2(f)]. LDI is the integrated value at the ground surface. The major procedures to calculate the LDI using SPT data are similar to those described above, although the profile may be less detailed than that produced from CPT data.

Although LDI has the units of displacement, it is intended only to provide an index to quantify potential lateral displacements for a given soil profile, soil properties, and earthquake characteristics. The actual magnitude of lateral displacement depends on both LDI and geometric parameters characterizing ground geometry. In the following sections, lateral spread case histories are used to account for the influence of ground geometry on lateral displacements.

Case Histories

A total of 13 available case histories associated with 12 past major earthquakes were studied as listed in Table 1. A summary of each case history and the rationale behind the selection of data for use in this paper can be found in Zhang (2001). Several case histories involving lateral spreads that were impeded by shear forces along the margins of the failure zone or by engineered structures (e.g., retaining walls, quay walls) were not used in this study. For example, data from the 1995 Hyogoken-Nambu (Kobe) earthquake were not used in this study since lateral spreading in the Port area was believed to be greatly restricted by caisson-type quay walls (Zhang 2001). Lateral spreads that were possibly associated with multiple failure mechanisms (e.g., several case sites from the 1994 Northridge Earthquake) were also not included in the database either. The possibility of local slump failure or flow failure increases in the zone close to a free face with a steep slope due to the presence of high static shear stresses. Further, the mechanism associated with a local slump failure or flow failure is fundamentally different from that for lateral spreading. Therefore some case sites (e.g., Sandholdt Road at Moss Landing) where the horizontal distance from the free face toe is smaller than four times the free face height were excluded from the database. Selection of cases also required that SPT or CPT data were available at locations within 100 m of where liquefaction-induced lateral displacement was measured. Case histories were divided into those with: (1) gently sloping ground without a free face, (2) nearly level ground with a free face, and (3) gently sloping ground with a free face.

A total of 291 measured values of liquefaction-induced lateral spreading displacements from the 13 case histories were used in this study. There were usually more than one distinct lateral spread features/sites for each case history studied, as listed in Tables 2–4. Multiple lateral displacements with different mea-

Table 1. Cases Selected for Database on Liquefaction Lateral Spreads

Case	References	Liquefied soil description	Liquefied soil thickness (m)
Hokkaido 1993	Isoyama (1994)	Silty sand with about 10% fines	4.5–5.5
Dagupan 1990	Wakamatsu et al. (1992); Ishihara et al. (1993); Tokimatsu et al. (1994)	Fine clean sand and silty sand	5.1–8.6
Moss Landing 1989	O'Rourke and Pease (1992); Boulanger et al. (1995, 1997); Mejia (1998)	Clean sand and silty sand	0.8–5.2
Wildlife 1987	Bennett et al. (1984); Holzer et al. (1989); Youd and Bartlett (1988); Dobry et al. (1992)	Silty sand or sandy silt with 17–50% fines	0.5–2.7
Noshiro 1983	Hamada et al. (1986); Bartlett (1991); Hamada (1992b)	Clean dune sand and alluvial sand	1.0–7.0
Heber Road 1979	Bennett et al. (1981); Norton (1983); Youd and Bennett (1983); Dobry et al. (1992)	Channel sand with 14–37% fines	0.0–5.3
Juvenile Hall 1971	Bennett (1989); O'Rourke et al. (1992b)	Alluvium with 50–80% fines	0.9–3.0
Jensen Plant 1971	O'Rourke et al. (1992b)	Alluvium with 32–62% fines	0.0–7.7
Niigata 1964	Bartlett (1991); Hamada (1992a); Bartlett and Youd (1995); Hamada et al. (1986)	Mainly clean, fine or medium sands	0.6–18.1
Alaska 1964	Bartlett (1991); Bartlett and Youd (1995); McCulloch and Bonilla (1970)	Sand and gravel, silty sand, sandy silt	4.0–9.4
Fukui 1948	Hamada et al. (1992b); Rauch (1997)	Silt, silty sand, sand, sandy gravel	1.7–5.7
Kanto 1923	Hamada et al. (1992a); Rauch (1997)	Fine sand with about 10% fines	8.0–8.8
San Francisco 1906	Pease and O'Rourke (1993, 1998); O'Rourke et al. (1992a); Youd and Hoose (1976, 1978)	Relatively clean dune sand	1.3–8.5

sured values at a given case site were collected for most of the case histories. These points corresponded to either different local ground geometric parameters or soil profile/properties. The minimum spacing of any two points collected for this study was about 20 m or more. Measurements of lateral displacement that were deemed to be too close to the boundaries of a lateral spread were not included in the database.

In situ test results from 150 SPTs and 41 CPTs associated with the studied case histories were collected. Of the 13 case histories, SPT data were available for nine of the cases and CPT data were available only for five of the cases. The case history data were collected from the available publications as listed in Table 1. Partial data, especially for the 1964 Niigata earthquake, were obtained from the database compiled by Bartlett (1991).

In most cases the magnitude of lateral displacement were obtained from aerial photos that were taken before and after the earthquake or from reports of dislocated or offset buildings, bridge components, fences, canals, etc. The estimated values of accuracy (or potential error) associated with the measured displacements are also given in Tables 2–4.

Correlation between Actual Lateral Displacement, Lateral Displacement Index, and Geometric Parameters

Gently Sloping Ground without a Free Face

Cases with Standard Penetration Test Data

A total of five case histories with SPT data were studied for the case of gently sloping ground without a free face, as listed in Table 2. The corresponding measured lateral displacement values or ranges are also listed and are labeled LD. For each case, the NCEER SPT-based method was applied to evaluate liquefaction potential using SPT data. The lateral displacement index (LDI) was then calculated based on the results of the liquefaction potential analysis, the relationship in Fig. 1, and using Eq. (3). An average of the calculated values of LDI was used as a representative LDI value if more than one SPT profile was conducted close to where LD was measured. A total of 132 data sets were obtained from the five case histories with SPT data.

Table 2. Cases with Gently Sloping Ground without a Free Face

Case history	Noshiro 1983	Juvenile Hall 1971	Niigata 1964	Fukui 1948	Kanto 1923	San Francisco 1906
Number of sites	3	1	3	2	1	2
Number of LD data	23	1	103	4	1	8
LD (cm)	65–298	168	80–460	100–350	250	60–210
Accuracy of LD (\pm cm)	17	2	72	190	>50	10–50
LDI (cm)	17–164	60 SPT 18 CPT	37–538	19–250	184–232	33–173
S (%)	0.2–7.5	1.2	0.2–0.9	0.4–3.4	1.6	1.0–2.3
M_w	7.7	6.4	7.5	7.0	7.9	7.9
a_{max} (g)	0.25	0.55	0.19	0.25	0.25	0.6
Number of SPT and CPT	21 SPT	5 SPT 5 CPT	27 SPT	3 SPT	2 SPT	17 CPT

Note: LD=lateral displacement; LDI=lateral displacement index; SPT=standard penetration test; and CPT=cone penetration test.

Table 3. Cases with Nearly Level Ground and a Free Face

Case history	Moss		Jensen		Alaska
	Dagupan 1990	Landing 1989	Plant 1971	Niigata 1964	
Number of sites	3	2	1	2	1
Number of LD data	7	6	13	66	1
LD (cm)	50–600	30–125	2–100	41–1015	157
Accuracy of LD (±cm)	>50	>10	47	72	10–50
LDI (cm)	79–220	28–114	5–20	246–637	173
<i>H</i> (m)	4–11.5	1.9–2.4	10.4–17.2	4.9–5.2	4.9
<i>L/H</i>	3.8–27.3	6.3–23.5	8.7–30.5	5.1–36.2	6.2
<i>M_w</i>	7.6	7.0	6.4	7.5	9.2
<i>a_{max}</i> (g)	0.2	0.25	0.55	0.19	0.31
Number of SPT and CPT	3 (SPT)	7 (CPT)	20 (SPT)	47 (SPT)	3 (SPT)

Note: LD=lateral displacement; LDI=lateral displacement index; SPT =standard penetration test; and CPT=cone penetration test.

Fig. 3(a) is a plot of LD/LDI versus ground slope *S* for the five case histories. The ground slope is defined as the average gradient over relatively long (20 m or more) ground with a similar general gradient. A general trend of increasing LD/LDI with increasing ground slope can be seen from Fig. 3(a) that can be expressed as

$$\frac{LD}{LDI} = S + 0.2 \quad (\text{for } 0.2\% < S < 3.5\%) \quad (4)$$

where *S*=ground slope as a percentage.

A dominant portion (95%) of the data in Fig. 3(a) was collected from two Japanese case histories (Niigata and Noshiro). The liquefied soils at these sites were generally clean sands. Because the ground slopes at all the sites for the Niigata case history were between 0.2 and 0.9% and with an average of about 0.5%, the data for this case history dominates the trend line in Fig. 3(a) for a ground slope less than 1%. The data for the Noshiro case history dominates the relationship in Fig. 3(a) for a ground slope greater than 1%, especially for a ground slope greater than 3.5%. The data from the other three case histories generally fits well with the relationship in Fig. 3(a) for ground slopes ranging from about 0.5 to 3.5%. Given the exclusive reliance on the Noshiro case history for ground slopes greater than 4%, the recommended range of ground slope for Eq. (4) is between 0.2 and 3.5%.

Table 4. Cases with Gently Sloping Ground and a Free Face

Case history	Heber		Niigata	
	Hokkaido 1993	Wildlife 1987		Road 1979
Number of sites	1	1	1	1
Number of LD data	6	3	17	32
LD (cm)	96–286	11–18	30–424	67–617
Accuracy of LD (±cm)	22	2	10–50	72
LDI (cm)	130–210	24–35	82–192	78–402
<i>S</i> (%)	0.7, 0.8	–0.47	1.5	–0.34–0.48
<i>H</i> (m)	1.9–2.5	2.4	1.6	3.4–5.2
<i>L/H</i>	17–36	6.9–10.2	7.6–25	4.9–37.3
<i>M_w</i>	7.7	6.5	6.5	7.5
<i>a_{max}</i> (g)	0.25	0.21	0.6	0.19
Number of SPT and CPT	4 (SPT)	4 (CPT)	8 (CPT)	15 (SPT)

Note: LD=lateral displacement; LDI=lateral displacement index; SPT =standard penetration test; and CPT=cone penetration test.

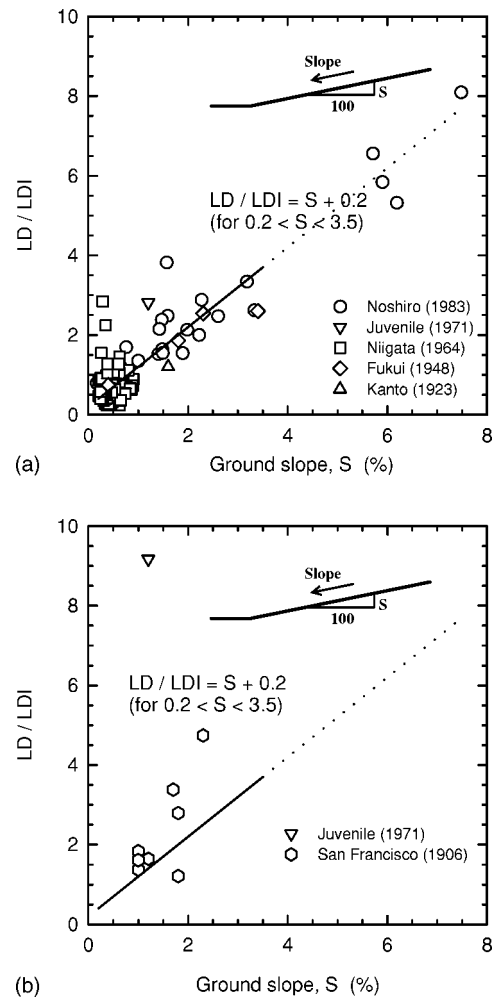
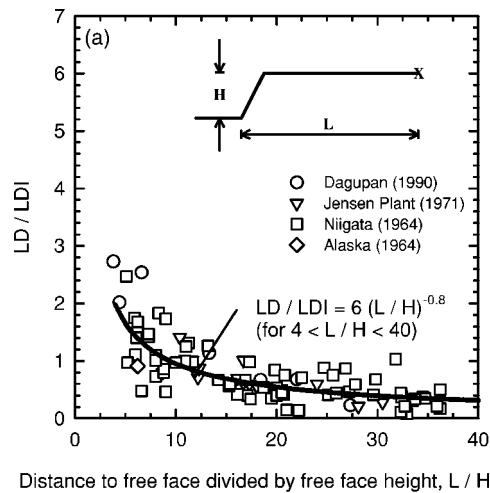


Fig. 3. Ratio of measured lateral displacement lateral displacement (LD) to lateral displacement index lateral displacement index (LDI) versus ground slope *S* for case histories with gently sloping ground without a free face: (a) standard penetration test-based data and (b) cone penetration test-based data

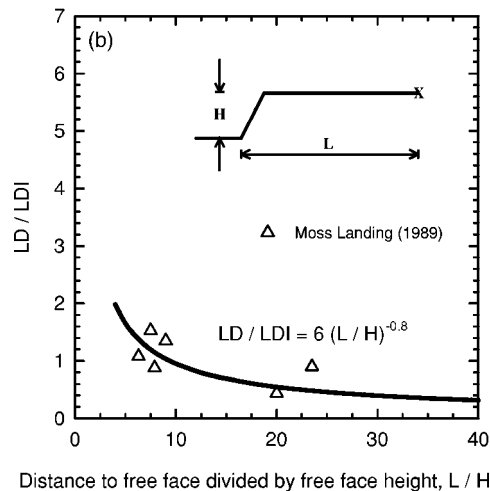
Cases with Cone Penetration Test Data

San Francisco and Juvenile Hall are two cases with CPT data and gently sloping ground without a free face. Eight data points were obtained for the San Francisco case history. Only one set of data was obtained for the Juvenile Hall case history because of a uniform measured lateral displacement of 1.68 m and a ground slope of 1.2% at the main part of the lateral spreading section where most of the penetration tests were conducted. Fig. 3(b) is a plot of LD/LDI versus ground slope *S* for the 9 CPT-based data sets as well as the trend line that was developed above based on SPT-based data.

The point from the Juvenile Hall case history associated with the 1971 San Fernando earthquake is far removed from the trend line in Fig. 3(b). It is believed that the main reason for this inconsistency is because the NCEER CPT-based method generally treats soils with a soil behavior type index *I_c* greater than 2.6 as nonliquefiable. The soil behavior type index is calculated from CPT data and provides an index of the soil grain characteristics (Robertson and Wride 1998). An *I_c* equal to 2.6 corresponds to a calculated fines content of about 50–60% (Zhang 2001). Since Bennett (1989) reported that the fines contents for the liquefied soils at the Juvenile Hall case site ranged from 50 to 80% with an average of 65%, this implies that the majority of the liquefied



Distance to free face divided by free face height, L/H



Distance to free face divided by free face height, L/H

Fig. 4. Ratio of measured lateral displacement lateral displacement (LD) to lateral displacement index lateral displacement index (LDI) versus L/H for case histories with level ground and a free face: (a) standard penetration test-based data and (b) cone penetration test-based data

soils in the Juvenile Hall area may have a calculated I_c greater than 2.6 and thus would be evaluated as nonliquefiable soils by the NCEER CPT-based method. This would result in a smaller calculated value of LDI and thus a higher value of LD/LDI, as shown in Fig. 3(b). As suggested by Robertson and Wride (1998), samples of soil should be obtained for I_c greater than 2.6 and liquefaction evaluated using the other criteria, such as the Chinese criteria (NCEER 1997). Therefore the point in Fig. 3(b) for the Juvenile Hall site may be ignored in qualifying the correlation between LD/LDI and ground slope using CPT data, and illustrates the caution required with assessing liquefaction potential for soils with I_c greater than 2.6.

Fig. 3(b) shows that the data for the San Francisco case history associated with the 1906 San Francisco earthquake reasonably fit the trend line obtained from SPT data with some scatter. This agreement may suggest that the relationship between LD/LDI and ground slope is independent of either using SPT or CPT data and possibly that it solely captures the influence of ground slope on lateral displacements. This is encouraging, however, additional CPT-based data from new case histories are required to further verify this observation.

Level Ground with a Free Face

In this study, terrain with a slope of less than 0.15% is defined as “level” ground. Two major geometric parameters characterizing ground geometry for level ground with a free face are free face height H , which is the elevation difference between the level ground surface and the toe of a free face, and the horizontal distance L from the toe of a free face (see the inset of Fig. 4). Bartlett (1991) observed from case histories that lateral displacements were greater closer to a free face and for higher free faces. Similar trends were observed at the Kobe Port area during the 1995 Hyogoken-Nambu earthquake (Ishihara et al. 1996) even though these lateral displacements are believed to have been restricted by quay walls. The ratio of L/H was adopted to establish a correlation between LD and LDI for level ground with a free face.

Cases with Standard Penetration Test Data

Four case histories with SPT data for level ground conditions with a free face are available, as listed in Table 3. A total of 87 data points from the four case histories associated with four different earthquakes are plotted in Fig. 4(a). The data in Fig. 4(a) is predominantly from the 1964 Niigata case history, however, the results from the other case histories generally follow the same trend. Although there is considerable scatter, Fig. 4(a) shows a trend of decreasing LD/LDI with increasing L/H that may be characterized by

$$\frac{LD}{LDI} = 6 \cdot \left(\frac{L}{H}\right)^{-0.8} \quad (\text{for } 4 < L/H < 40) \quad (5)$$

This general trend is applicable for the range of earthquake and ground conditions listed in Table 3.

Case with Cone Penetration Test Data

Fig. 4(b) is a plot of LD/LDI versus L/H based on the data from the Moss Landing case history, which is the only case with CPT data and level ground conditions with a free face that qualified for this study. The data in Fig. 4(b) suggests that the trend line developed based on the SPT-based data reasonably fits the CPT-based data from the Moss Landing case history.

The intent of the empirical relationship of Eq. (5) is to account for the influence of the height and location of the free face on lateral displacement. The good agreement between the SPT-based and CPT-based data may suggest that Eq. (5) may be independent of either using SPT or CPT data (provided that NCEER procedures are used for liquefaction potential evaluation). It is possible that this relationship solely captures the influence of H and L on lateral displacements. This preliminary observation is encouraging, however, additional data, especially CPT-based data from new case histories, is required to further evaluate this observation.

Gently Sloping Ground with a Free Face

Four cases were available for gently sloping ground with a free face. In addition to the free face height and the distance from the free face, ground slope S is required to characterize the geometry of the site (Fig. 5). A positive ground slope is inclined towards the free face (e.g., a channel) whereas a negative ground slope is inclined away from the free face.

Table 4 provides a summary of the main parameters for these cases. SPT results were available for two cases, and CPT results were available for the other two cases. Since the relationship between LD/LDI and geometric parameters appears to be indepen-

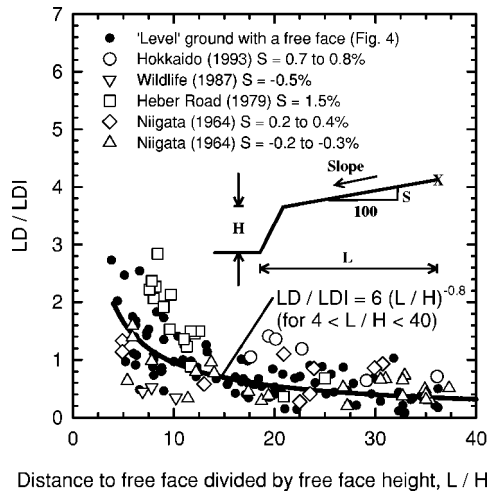


Fig. 5. Ratio of measured lateral displacement (LD) to lateral displacement index (LDI) versus L/H for case histories for level and gently sloping ground with a free face

dent of either using SPT-based or CPT-based data, SPT and CPT cases are combined together to provide a larger data set.

Fig. 5 illustrates the relationship between LD/LDI and L/H using both the SPT- and CPT-based data for the four available case histories for gently sloping ground with a free face. The datapoints from Figs. 4(a and b) are also included in Fig. 5 to provide a comparison with nearly level ground and a free face.

The data points for gently sloping ground and a free face lie generally within the scatter of results for nearly level ground with a free face. It appears that a negative slope decreases LD/LDI as

the results from the Wildlife case ($S = -0.5\%$) lie toward the lower range of the scatter. Larger positive slopes tend to increase LD/LDI , as the results for the Heber Road ($S = 1.5\%$) and Hokkaido ($S = 0.7$ to 0.8%) cases lie toward the upper range of the scatter. Thus the ground slope appears to influence the magnitude of lateral displacements, however, there is insufficient data at present to quantify this effect. Caution is required to estimate liquefaction-induced lateral displacements for gently sloping ground with slopes greater than 0.5% .

Proposed Approach to Estimate Lateral Displacements Using Standard Penetration Test or Cone Penetration Test Data

The following method may be used to estimate liquefaction induced lateral displacements.

Step 1: Assess the liquefaction potential using either the NCEER SPT- or CPT-based methods.

Step 2: Calculate the lateral displacement index (LDI) using the relationship plotted in Fig. 1 and Eq. (3).

Step 3: Knowing ground slope (S) or/and free face height (H) and the distance to a free face (L), estimate the lateral displacement (LD) using either

$$LD = (S + 0.2) \cdot LDI \quad (\text{for } 0.2\% < S < 3.5\%) \quad (6)$$

for gently sloping ground without a free face, or

$$LD = 6 \cdot (L/H)^{-0.8} \cdot LDI \quad (\text{for } 4 < L/H < 40) \quad (7)$$

for level ground with a free face.

The proposed approach is recommended for use within the ranges of earthquake properties and ground conditions listed in Tables 2–4, namely moment magnitude of earthquake between

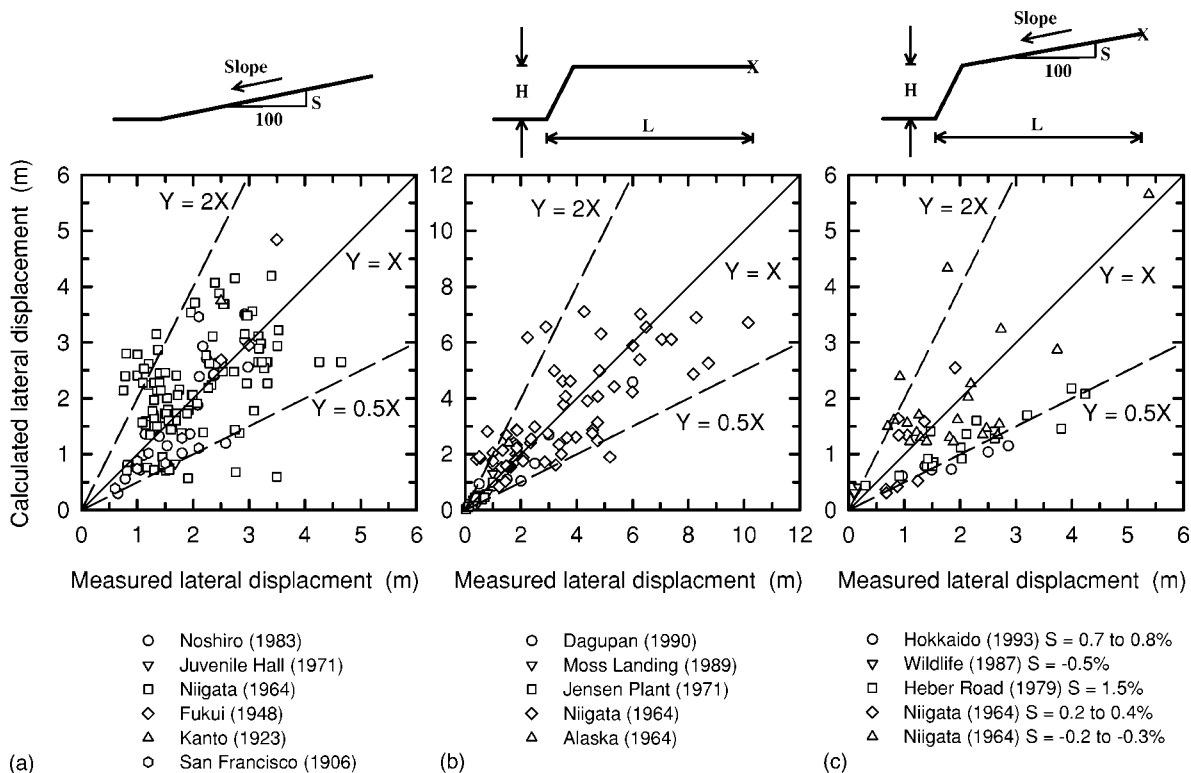


Fig. 6. Comparison of measured and calculated lateral displacements for the available case histories for: (a) gently sloping ground without a free face; (b) level ground with a free face; and (c) gently sloping ground with a free face

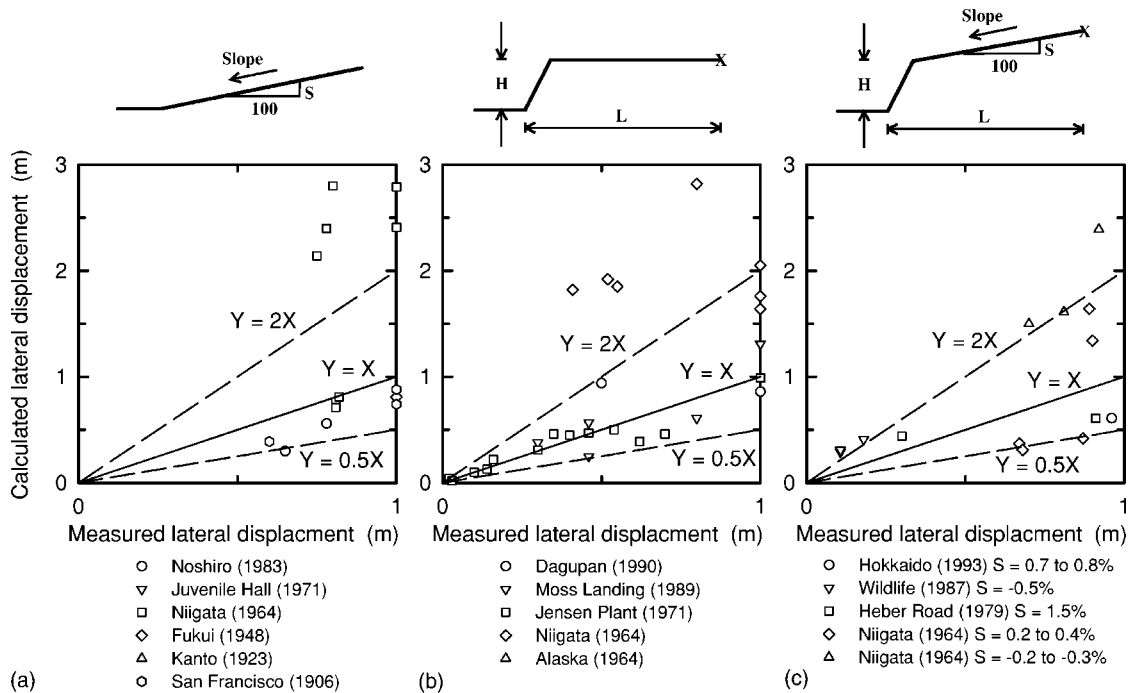


Fig. 7. Comparison of measured lateral displacements less than 1 m and calculated lateral displacements for the available case histories for: (a) gently sloping ground without a free face; (b) level ground with a free face; and (c) gently sloping ground with a free face

6.4 and 9.2, peak surface acceleration between $0.19g$ and $0.6g$, and free face heights less than 18 m. The case history data used for developing the proposed approach, especially for gently sloping ground without a free face, were dominantly from two Japanese case histories associated with the 1964 Niigata and 1983 Nihonkai-Chubu earthquakes, where the liquefied soils were mainly clean sand only. The values for the geometric parameters used in developing the proposed approach were within limited ranges, as specified in Eqs. (6) and (7). It is recommended that the approach not be used when the values of the geometric parameters go beyond the specified ranges.

Caution should also be exercised when a substantial zone of soil with a very low value penetration resistance [i.e., $(N_1)_{60cs} < 10$ or $(q_{c1N})_{cs} < 50$] is encountered during liquefaction potential analysis. For such cases, more extensive investigation should be made and other approaches should be taken to evaluate the potential for flow failure of the soil, especially when the static shear stresses in the ground are relatively high. Deformations caused by flow failures can be much larger than those by lateral spreads, and their estimation is beyond the scope of this paper.

Discussion

Variability of the Proposed Approach

Measured lateral displacements from the available case histories are compared with the calculated lateral displacements using the proposed approach in Fig. 6. Generally, about 90% of the calculated lateral displacements using the proposed approach showed variations between 50 and 200% of measured values for the case histories studied. The proposed approach could underestimate or overestimate liquefaction-induced lateral displacements by up to a factor of 2. The accuracy of the calculated displacements for the Niigata case history is slightly lower than that for other case

histories because of the relatively poor accuracy (± 0.72 m) of the measured displacements and relatively flat ground slopes (0.2 – 0.9%), where local topography variations and/or the presence of buildings may have more significant effects on lateral displacements than those for steeper slopes.

Given the complexity of liquefaction-induced lateral spreads, considerable variations in magnitude and distribution of lateral displacements at a given site are expected. Considering the accepted ability of current calculations of ground settlements in sand for the simple case of static vertical loading, the accuracy of the proposed approach may be reasonable and acceptable at the current stage for low to medium risk projects.

Small Lateral Displacements

Often of practical interest is whether lateral displacements at a site will be sufficiently small such that they will not have a detrimental effect on a structure. Fig. 7 is an enlarged portion of Fig. 6 to better show the variability of the proposed approach when measured lateral displacements are less than 1 m. In all cases it is not possible to make definitive conclusions given the small number of measured displacements less than 1 m and there is no information for gently sloping ground with measured displacements less than 0.5 m. However, apart from nine observations associated with Niigata, the predicted lateral displacements are generally within 50–200% of the measured values. Thus if the calculated lateral displacement using the proposed approach was 1 m, it would not be possible to conclude that the displacement would be 1 m, but rather may be expected to vary between 0.5 and 2 m. Further, given the accuracy of the measured lateral displacements for most case histories ranges from ± 0.1 to ± 1.92 m (see Tables 2–4), it is therefore unrealistic to expect the accuracy of calculated lateral displacements to be less than ± 0.1 m.

Comparison of Proposed Approach with Youd et al. (2002)

Several SPT-based models (Rauch and Martin 2000; Youd et al. 2002) are currently available to estimate liquefaction-induced lateral displacements. Rauch and Martin's empirical method was developed using case history data from a multiple linear regression analysis. However, it can only be used to estimate an average value of lateral displacements on a potential lateral spread. The model of Youd et al. (2002) was developed using multiple linear regression techniques and case history data including seismological, topographical, geological, and geotechnical parameters. Although their method is very simple and straightforward to use, the method is purely empirical, does not build upon liquefaction potential analysis, and relies on using SPT-based average values for some input data.

Preliminary comparisons between the proposed approach and the model of Youd et al. (2002) indicated that the accuracy of these two methods were generally similar for estimating lateral displacements for gently sloping ground without a free face or level ground with a free face for the Niigata case history. Further evaluations are required using data from new case histories as they become available before a general conclusion can be made.

Assumptions, Limitations and Complicating Factors

Multiple displacements with different measured values at a given case site were collected for most of the case histories. These points corresponded to either different local ground geometric parameters or soil profile/properties and were included to evaluate the effects of local geometry and soil profile/properties under a given earthquake. However, their inclusion may bias the database to certain particular sites. The effect of this bias depends on the spread of the data and the method of analysis used to quantify the data. Approaches using multiple regression analysis would be biased since some observations may not necessarily be statistically independent. The approach adopted in this paper is to plot all of the available observations that met the screening criterion to show the trends and variability of the data. Relationships presented to quantify the trend in the database in this paper were fit by-eye rather than using regression analysis.

Moment magnitude of an earthquake (M_w) and peak surface acceleration (a_{max}) at a given site are used to characterize the earthquake size and the intensity of strong ground motion in this approach. Other earthquake characteristics (e.g., the duration of strong motion and the distance to a seismic energy source or fault rupture) are believed to inherently correlate with M_w and a_{max} . Generally, the higher values of M_w and a_{max} will result in lower values of FS and thicker zones of liquefied soil, resulting in higher values of LDI. It is implicitly assumed that the effects of earthquake characteristics on lateral spreading displacements can be quantified by their effects on FS and thickness of liquefied soils or LDI. This assumption is tenable based on the available data as no biased trends were identified from the case history data shown in Figs. 3 and 4 for different earthquakes with wide ranges of properties (M_w from 6.4 to 7.7 and a_{max} from 0.19g to 0.55g). However, given the limited number of cases, further evaluation of the influence of earthquake characteristics is needed once additional data becomes available.

It is also assumed in this paper that the effect of fines content on lateral spreading is similar to that on liquefaction triggering. No discernable trend between fines content and lateral displacement was observed based on the available data shown in Figs. 3

and 4. Future research is needed to further verify this assumption with new data as it becomes available.

The proposed approach was developed using the limited data from available case histories and as such is applicable only for similar earthquakes and ground conditions. In situ CPT data were available only for five of all the case histories studied in this paper. Therefore additional case history data, especially with CPT data, are required to evaluate the proposed approach. In addition, the proposed approach was developed based on data with limited ranges. More data from new case histories are needed to update the proposed approach.

Several factors including boundaries and three-dimensional distribution of liquefied layers, redistribution and drainage of excess pore pressures in a lateral spread, and isolation of acceleration due to liquefaction of underlying soil layers may also influence liquefaction-induced lateral displacements (Zhang 2001). However, they were not quantified in the proposed approach and would need to be evaluated on a case-by-case basis.

Conclusions

An approach to estimate liquefaction-induced lateral spreading displacements was presented. The proposed approach uses either SPT or CPT data and combines results from laboratory tests with case history data from previous earthquakes. The method captures the mechanisms of liquefaction-induced lateral spreads and characterizes the major factors controlling lateral displacements. Application of the proposed method is quite simple and can be applied with only a few additional calculations following SPT- or CPT-based liquefaction-potential analysis. The proposed approach may be suitable to estimate the magnitude of lateral displacements associated with liquefaction-induced lateral spread for gently sloping (or level) ground with or without a free face for low to medium-risk projects, or to provide preliminary estimates for higher risk projects.

Given the complexity of liquefaction-induced lateral spreads, considerable variations in magnitude and distribution of lateral displacements are expected. Generally, the calculated lateral displacements using the proposed approach for the available case histories showed variations between 50 and 200% of measured values. The accuracy of "measured" lateral displacements for most case histories is about ± 0.1 to ± 1.92 m. Therefore it is unrealistic to expect the accuracy of estimated lateral displacements be within ± 0.1 m. The reliability of the proposed approach can be fully evaluated only over time with more available case histories.

The proposed approach was developed using case history data with limited ranges of earthquake parameters, soil properties, and geometric parameters. Therefore it is not recommended that the approach be applied for values of input parameters beyond the specified ranges. Engineering judgement and caution should be always exercised in applying the proposed approach and in interpreting the results. Additional new data are required to further evaluate and update the proposed approach.

Acknowledgments

This research was funded by the Natural Science and Engineering Research Council of Canada (NSERC). Financial support was also provided by the University of Alberta to the first writer through FS Chia PhD and Coal Mining Research Company Scholarships. The lateral spread database compiled by Dr. S. F.

Bartlett and later then published by Dr. T. L. Youd of Brigham Young University on the world wide web for researchers to download was a highly valuable source of case history data.

Appendix. Relationship between Maximum Cyclic Shear Strain and Factor of Safety

The mathematic expressions for the curves in Fig. 1 are

$$\text{if } D_r=90\%, \quad \gamma_{\max}=3.26(\text{FS})^{-1.80} \quad \text{for } 0.7 \leq \text{FS} \leq 2.0 \quad (8)$$

$$\text{if } D_r=90\%, \quad \gamma_{\max}=6.2 \quad \text{for } \text{FS} \leq 0.7 \quad (9)$$

$$\text{if } D_r=80\%, \quad \gamma_{\max}=3.22 \cdot (\text{FS})^{-2.08} \quad \text{for } 0.56 \leq \text{FS} \leq 2.0 \quad (10)$$

$$\text{if } D_r=80\%, \quad \gamma_{\max}=10 \quad \text{for } \text{FS} \leq 0.56 \quad (11)$$

$$\text{if } D_r=70\%, \quad \gamma_{\max}=3.20 \cdot (\text{FS})^{-2.89} \quad \text{for } 0.59 \leq \text{FS} \leq 2.0 \quad (12)$$

$$\text{if } D_r=70\%, \quad \gamma_{\max}=14.5 \quad \text{for } \text{FS} \leq 0.59 \quad (13)$$

$$\text{if } D_r=60\%, \quad \gamma_{\max}=3.58 \cdot (\text{FS})^{-4.42} \quad \text{for } 0.66 \leq \text{FS} \leq 2.0 \quad (14)$$

$$\text{if } D_r=60\%, \quad \gamma_{\max}=22.7 \quad \text{for } \text{FS} \leq 0.66 \quad (15)$$

$$\text{if } D_r=50\%, \quad \gamma_{\max}=4.22 \cdot (\text{FS})^{-6.39} \quad \text{for } 0.72 \leq \text{FS} \leq 2.0 \quad (16)$$

$$\text{if } D_r=50\%, \quad \gamma_{\max}=34.1 \quad \text{for } \text{FS} \leq 0.72 \quad (17)$$

$$\text{if } D_r=40\%, \quad \gamma_{\max}=3.31 \cdot (\text{FS})^{-7.97} \quad \text{for } 1.0 \leq \text{FS} \leq 2.0 \quad (18)$$

$$\text{if } D_r=40\%, \quad \gamma_{\max}=250 \cdot (1.0 - \text{FS}) + 3.5 \quad \text{for } 0.81 \leq \text{FS} \leq 1.0 \quad (19)$$

$$\text{if } D_r=40\%, \quad \gamma_{\max}=51.2 \quad \text{for } \text{FS} \leq 0.81 \quad (20)$$

Notation

The following symbols are used in this paper:

- a_{\max} = peak surface acceleration;
- D_r = relative density of a clean sand as a percentage;
- FS = factor of safety against liquefaction;
- H = free face height;
- I_c = soil behavior type index;
- L = horizontal distance from the toe of a free face;
- LD = actual lateral displacement;
- LDI = lateral displacement index;
- M_w = moment magnitude of earthquake;
- $(N_1)_{60}$ = corrected normalized SPT N value;
- $(N_1)_{60cs}$ = equivalent clean sand normalized SPT N value;
- q_c = CPT tip resistance;
- q_{c1N} = corrected normalized CPT tip resistance;
- $(q_{c1N})_{cs}$ = equivalent clean sand normalized CPT penetration resistance;
- R_f = CPT sleeve friction ratio;
- S = ground slope;
- Z_{\max} = maximum depth of potential liquefiable layers with a calculated $\text{FS} < 2.0$ at a studied site;
- z = depth below ground surface; and
- γ_{\max} = maximum amplitude of cyclic shear strain.

References

Abdoun, T. H. (1997). "Modeling of seismically induced lateral spreading of multi-layered soil and its effect on pile foundations." PhD

- thesis, the Rensselaer Polytechnic Institute, Troy, N.Y.
- Bardet, J. P., Tobita, T., Mace, N., and Hu, J. (2002). "Regional modeling of liquefaction-induced ground deformation." *Earthquake Spectra*, 18(1), 19–46.
- Bartlett, S. F. (1991). "Empirical analysis of horizontal ground displacement generated by liquefaction-induced lateral spreads." PhD thesis, Brigham Young Univ., Provo, Utah.
- Bartlett, S. F., and Youd, T. L. (1995). "Empirical prediction of liquefaction-induced lateral spread." *J. Geotech. Eng.*, 121(4), 316–329.
- Bennett, M. J. (1989). "Liquefaction analysis of the 1971 ground failure at the San Fernando Valley Juvenile Hall, California." *Bull. Assoc. Eng. Geologists*, XXVI(2), 209–226.
- Bennett, M. J., McLaughlin, P. V., Sarmiento, J. S., and Youd, T. L. (1984). "Geotechnical investigation of liquefaction sites, Imperial Valley, California." *Open-File Rep. 84-252*, U.S. Geological Survey, Menlo Park, Calif., 103.
- Bennett, M. J., Youd, T. L., Harp, E. L., and Wieczorek, G. F. (1981). "Subsurface investigation of liquefaction, Imperial Valley Earthquake, California, October 15, 1979." *Open-File Rep. 81-502*, U.S. Geological Survey, Menlo Park, Calif., 83.
- Boulanger, R. W., Idriss, I. M., and Mejia, L. H. (1995). "Investigation and evaluation of liquefaction related ground displacements at Moss Landing during the 1989 Loma Prieta earthquake." *Rep. No. UCD/CGM-95/02*, Dept. of Civil & Environmental Engineering, Univ. of California at Davis, Davis, Calif.
- Boulanger, R. W., Mejia, L. H., and Idriss, I. M. (1997). "Liquefaction at Moss Landing during Loma Prieta earthquake." *J. Geotech. Geoenviron. Eng.*, 123(5), 453–467.
- Dobry, R., Baziar, M. H., O'Rourke, T. D., Roth, B. L., and Youd, T. L. (1992). "Liquefaction and ground failure in the Imperial Valley, Southern California, during the 1979, 1981 and 1987 earthquakes. Case Studies of Liquefaction and Lifeline Performance during Past Earthquakes, Vol. 2." *Technical Rep. NCEER-92-0002*, 4-1–4-84.
- Elgamal, A., Dobry, R., Parra, E., and Yang, Z. (1998). "Soil dilation and shear deformations during liquefaction." *Proc., Fourth Int. Conf. on Case Histories in Geotechnical Engineering*, St. Louis, 1238–1259.
- Hamada, M. (1992a). "Large ground deformations and their effects on lifelines: 1964 Niigata earthquake. Case Studies of Liquefaction and Lifeline Performance During Past Earthquake, Vol. 1." *Technical Rep. NCEER-92-0001*, National Center for Earthquake Engineering Research, Buffalo, N.Y., 3-1–3-123.
- Hamada, M. (1992b). "Large ground deformations and their effects on lifelines: 1983 Nihonkai-Chubu earthquake. Case Studies of Liquefaction and Lifeline Performance During Past Earthquake, Vol. 1." *Technical Rep. NCEER-92-0001*, National Center for Earthquake Engineering Research, Buffalo, N.Y., 4-1–4-85.
- Hamada, M., and O'Rourke, T. D. (1992). "Case studies of liquefaction and lifeline performance during past earthquakes. Volume 1, Japanese Case Studies." *Technical Rep. NCEER-92-0001*, National Center for Earthquake Engineering Research, Buffalo, N.Y.
- Hamada, M., Wakamatsu, K., and Yasuda, S. (1992a). "Liquefaction-induced ground deformation during the 1923 Kanto earthquake. Case studies of liquefaction and lifeline performance during past earthquakes, Vol. 1." *Technical Rep. NCEER-92-0001*, National Center for Earthquake Engineering Research, Buffalo, N.Y.
- Hamada, M., Yasuda, S., Isoyama, R., and Emoto, K. (1986). *Study on liquefaction induced permanent ground displacements*, Association for the Department of Earthquake Prediction in Japan, Tokyo, 87.
- Hamada, M., Yasuda, S., and Wakamatsu, K. (1992b). "Large ground deformations and their effects on lifelines: 1948 Fukui earthquake. Case Studies of Liquefaction and Lifeline Performance During Past Earthquakes, Vol. 1." *Technical Rep. NCEER-92-0001*, National Center for Earthquake Engineering Research, Buffalo, N.Y.
- Holzer, T. L., Youd, T. L., and Bennett, M. J. (1989). "In situ measurement of pore pressure build up during liquefaction." *Proc., 20th Joint Meeting of the U.S.—Japan Cooperative Program in the National Resources*, Panel on Wind and Seismic Effects, U.S. Department of Commerce.

- Ishihara, K., Acacio, A., and Towhata, I. (1993). "Liquefaction-induced ground damage in Dagupan in the July 16, 1990 Luzon earthquake." *Soils Found.*, 33(1), 133–154.
- Ishihara, K., Yoshida, K., and Kato, M. (1996). "Ground deformation characteristics caused by lateral spreading during the 1995 Hanshin-Awaji Earthquake." *Proc., 6th Japan-U.S. Workshop on Earthquake Resistant Design of Lifeline Facilities and Countermeasures for Soil Liquefaction*, Tech. Rep. NCEER-96-0012, 221–242.
- Ishihara, K., and Yoshimine, M. (1992). "Evaluation of settlements in sand deposits following liquefaction during earthquakes." *Soils Found.*, 32(1), 173–188.
- Isoyama, R. (1994). "Liquefaction-induced ground failures and displacements along the Shiribeshi-toshibetsu River caused by the 1993 Hokkaido-nansei-oki earthquake." *Proc., 5th U.S.-Japan Workshop on Earthquake Resistant Design of Lifeline Facilities and Countermeasures Against Soil Liquefaction*, Snowbird, Utah, Technical Rep. NCEER-94-0026.
- Jamiolkowski, M., Ladd, C. C., Germaine, J. T., and Lancellotta, R. (1985). "New developments in field and laboratory testing of soils." *Proc., 11th Int. Conf. on Soil Mechanics and Foundation Engineering*, San Francisco, Vol. 1, 57–153.
- Kulhawy, F. H., and Mayne, P. W. (1991). "Relative density, SPT and CPT interrelations." *Proc., 1st Int. Symp. on Calibration Chamber Testing*, ISCCCT1, Potsdam, N.Y., 197–211.
- Mejia, M. J. (1998). "Liquefaction at Moss Landing. The Loma Prieta, California, Earthquake of October 17, 1989—Liquefaction." *U.S. Geological Survey Professional Paper 1551-B*, B129–B150.
- Meyerhof, G. G. (1957). "Discussion on research on determining the density of sands." *Proc., 4th Int. Conf. of Soil Mechanics and Foundation Engineering*, London, Vol. 3, 110.
- McCulloch, D. S., and Bonilla, M. G. (1970). "Effects of the earthquake of March 27, 1964, on the Alaska railroad." *U.S. Geological Survey Professional Paper 545-D*.
- Nagase, H., and Ishihara, K. (1988). "Liquefaction-induced compaction and settlement of sand during earthquakes." *Soils Found.*, 28(1), 65–76.
- National Center for Earthquake Engineering Research (NCEER). (1997). *Proc., NCEER Workshop on Evaluation of Liquefaction Resistance of Soils*, T. L. Yound and I. M. Idriss, eds., Technical Rep. NCEER-97-0022, Salt Lake City.
- Norton, W. E. (1983). "In situ determination of liquefaction potential using the PQS probe." *Technical Rep. GL-83-15*, Geotechnical Laboratory, U.S. Army Engineer Waterways Experiment Station, Vicksburg, Miss.
- O'Rourke, T. D., Beaujon, P. A., and Scawthorn, C. R. (1992a). "Large ground deformations and their effects on lifeline facilities: 1906 San Francisco earthquake. Case studies of liquefaction and lifeline performance during past earthquakes, Vol. 2." *Technical Rep. NCEER-92-0002*, National Center for Earthquake Engineering Research, Buffalo, N.Y.
- O'Rourke, T. D., and Pease, J. W. (1992). "Large ground deformations and their effects on lifeline facilities: 1989 Loma Prieta Earthquake. Case studies of liquefaction and lifeline performance during past earthquakes, Vol. 2: United States case studies." *Technical Rep. NCEER-92-0002*, 5-1–5-79.
- O'Rourke, T. D., Roth, B. L., and Hamada, M. (1992b). "Large ground deformations and their effects on lifeline facilities: 1971 San Fernando earthquake. Case studies of liquefaction and lifeline performance during past earthquakes, Vol. 2." *Technical Rep. NCEER-92-0002*, National Center for Earthquake Engineering Research, Buffalo, N.Y.
- Pease, J. W., and O'Rourke, T. D. (1993). "Liquefaction hazards in the Mission District and South of Market areas, San Francisco, California. Liquefaction and ground failure in San Francisco: Site investigation, modeling, and hazard assessment for the urban environment." Grant No. 14-08-0001-G2128, Cornell Univ., Ithaca, N.Y.
- Pease, J. W., and O'Rourke, T. D. (1998). "Liquefaction hazards in the Mission District and South of Market area, San Francisco. The Loma Prieta, California, Earthquake of October 17, 1989—Liquefaction." *U.S. Geological Survey Professional Paper 1551-B*, B25–B60.
- Rauch, A. F. (1997). "EPOLLS: An empirical method for predicting surface displacements due to liquefaction-induced lateral spreading in earthquakes." PhD thesis, Virginia Polytechnic Institute and State Univ., Blacksburg, Va.
- Rauch, A. F., and Martin, J. R., II. (2000). "EPOLLS model for predicting average displacements on lateral spreads." *J. Geotech. Geoenviron. Eng.*, 126(4), 360–371.
- Robertson, P. K., and Wride, C. E. (1998). "Evaluating cyclic liquefaction potential using the CPT." *Can. Geotech. J.*, 35(3), 442–459.
- Sasaki, Y., Tokida, K., Matsumoto, H., and Saya, Y. (1991). "Shake table tests on lateral ground flow induced by soil liquefaction." *Proc., 3rd Japan-U.S. Workshop on Earthquake Resistant Design of Lifeline Facilities and Countermeasures for Soil Liquefaction*, San Francisco, CA, T. D. O'Rourke and M. Hamada, eds., National Center for Earthquake Engineering Research, SUNY-Buffalo, Buffalo, N.Y., 371–385.
- Seed, H. B. (1979). "Soil liquefaction and cyclic mobility evaluation for level ground during earthquakes." *J. Geotech. Eng. Div., Am. Soc. Civ. Eng.*, 105(2), 201–255.
- Skempton, A. K. (1986). "Standard penetration test procedures and the effects in sands of overburden pressure, relative density, particle size, aging and overconsolidation." *Geotechnique*, 36(3), 425–447.
- Taboada-Urtzuastegui, V. M., and Dobry, R. (1998). "Centrifuge modeling of earthquake-induced lateral spreading in sand." *J. Geotech. Geoenviron. Eng.*, 124(12), 1195–1206.
- Tatsuoka, F., Zhou, S., Sato, T., and Shibuya, S. (1990). "Method of evaluating liquefaction potential and its application." *Rep. on Seismic hazards in the soil deposits in urban areas*, Ministry of Education of Japan, 75–109 (in Japanese).
- Tokimatsu, K., Kojima, H., Kuwayama, S., Abe, A., and Midorikawa, S. (1994). "Liquefaction-induced damage to buildings in 1990 Luzon earthquake." *J. Geotech. Eng.*, 120(2), 290–307.
- Wakamatsu, K., Yoshida, N., Suzuki, N., and Tazoh, T. (1992). "Liquefaction-induced large ground deformations and their effects on lifelines during the 1990 Luzon, Philippines earthquake. Case Studies of Liquefaction and Lifeline Performance During Past Earthquakes, Vol. 1." *Technical Rep. NCEER-92-0001*, National Center for Earthquake Engineering Research, Buffalo, N.Y.
- Yasuda, S., Nagase, H., Kiku, H., and Uchida, Y. (1992). "The mechanism and a simplified procedure for the analysis of permanent ground displacement due to liquefaction." *Soils Found.*, 32(1), 149–160.
- Youd, T. L., et al. (2001). "Liquefaction resistance of soils: summary report from the 1996 NCEER and 1998 NCEER/NSF Workshops on evaluation of liquefaction resistance of soils." *J. Geotech. Geoenviron. Eng.*, 127(10), 817–833.
- Youd, T. L., and Bartlett, S. F. (1988). "US case histories of liquefaction-induced ground displacement." *1st Japan-United States Workshop on Liquefaction, Large Ground Deformation and Their Effects on Lifeline Facilities*, Tokyo, 22–31.
- Youd, T. L., and Bennett, M. J. (1983). "Liquefaction sites, Imperial Valley, California." *J. Geotech. Eng.*, 109(3), 440–457.
- Youd, T. L., Hansen, C. M., and Bartlett, S. F. (2002). "Revised multi-linear regression equations for prediction of lateral spread displacement." *J. Geotech. Geoenviron. Eng.*, 128(12), 1007–1017.
- Youd, T. L., and Hoose, S. N. (1976). "Liquefaction during 1906 San Francisco Earthquake." *J. Geotech. Eng.*, 102(5), 425–439.
- Youd, T. L., and Hoose, S. N. (1978). "Historic ground failures in Northern California triggered by earthquakes." *U.S. Geological Survey Professional paper 993*, U.S. Geological Survey.
- Zhang, G. (2001). "Estimation of liquefaction-induced ground deformations by CPT&SPT-based approaches." PhD thesis, Univ. of Alberta, Edmonton, Alta., Canada.